Key Engineering Materials Vols. 592-593 (2014) pp 313-316

doi:10.4028/www.scientific.net/KEM.592-593.313

Deformation mechanisms in ultrafine-grained Zn at different strain rates and temperatures

Péter Jenei[1, a], Guy Dirras[2, b], Jenő Gubicza[1, c], Hervé Couque[3, d]

[1] Department of Materials Physics, Eötvös Loránd University Budapest, P.O.B. 32, H-1518, Hungary

[2] Université Paris 13, Sorbonne Paris Cité, Laboratoire des Sciences, des Procédés et des Matériaux, 99, avenue Jean Baptiste Clément, 93430 Villetaneuse, France

[3] Nexter-Munitions, 7 route de Guerry, 18023 Bourges Cedex, France

[a]jeneip2@gmail.com, [b]dirras@univ-paris13.fr, [c]gubicza@metal.elte.hu, [d]h.couque@nexter-group.fr

Keywords: polycrystalline Zn; ultrafine grains; dynamic compression; indentation creep; strain rate sensitivity; twinning.

Abstract. The deformation mechanisms in ultrafine-grained hexagonal close packed Zn were investigated at different strain rates and temperatures. The influence of grain size on the deformation mechanisms was revealed by comparing the results obtained on ultrafine-grained and coarse-grained Zn. It was found that for coarse-grained Zn at room temperature and strain rates lower than 10^{-2} s^{-1} twinning contributed to plasticity besides dislocation activity. For strain rates higher than 10^{3} s^{-1} the plasticity in coarse-grained Zn was controlled by dislocation drag. In ultrafine-grained Zn the relatively large dislocation density (~10^{14} m^{-2}) and the small grain size (~250 nm) limit the dislocation velocity yielding the lack of dislocation drag effects up to 10^{4} s^{-1}. For ultrafine-grained Zn, twinning was not observed in the entire strain rate range due to its very small grain size. During room temperature compression at strain rates higher than 0.35 s^{-1} and in high temperature creep deformation of ultrafine-grained Zn besides prismatic <a> and pyramidal <c+a> dislocations observed in the initial state, <a>-type basal and pyramidal dislocations as well as other <c+a>-type pyramidal dislocations were formed.

Introduction

The deformation conditions, such as strain rate or temperature, and the microstructure have strong effect on the mechanisms of plasticity, thereby influencing the mechanical behavior of materials. For instance, in face centred cubic (FCC) materials the flow stress increases steeply when the strain rate is higher than about 10^{3} s^{-1} which is explained by a transition of deformation mechanism from thermally activated overcoming of obstacles by dislocations to viscous drag-controlled dislocation motion [1,2]. In coarse-grained hexagonal close-packed (HCP) metals, such as in Zn, the plastic deformation occurs via both twinning and dislocation slip when the samples subjected to compression at room temperature and low strain rates [3]. However, during compression at high strain rates twinning did not occur but rather significant grain refinement was observed, suggesting a transition to enhanced dislocation controlled plasticity [4]. The effect of the grain size on the deformation mechanisms in polycrystalline Zn submitted to quasistatic loading at room temperature has already been studied in details [4,5]. However, to the knowledge of the authors, the influence of the fine grain size on the mechanical behaviour of Zn at high strain rates or elevated temperatures have not been investigated yet. Therefore, in the present paper, the deformation mechanisms are studied in ultrafine-grained hexagonal Zn in a wide range of strain rate between 10^{-5} s^{-1} and 10^{4} s^{-1}. Additionally, the creep behavior in the temperature range of 330-359 ˚C is also investigated. The deformation mechanisms are determined from the changes of the microstructure during room temperature compression and high temperature creep tests.

Experimentals

High purity Zn powder (with an average particle size of 150 nm) was consolidated by Spark Plasma Sintering (SPS) to produce a bulk ultrafine-grained Zn (UFG-Zn) sample. The dwell time, the applied pressure and temperature of the SPS method were 5 min, 125 MPa and 300 ˚C, respectively. The deformation behavior of UFG-Zn sample was compared to the plastic properties of a high purity cast coarse-grained Zn sample (hereafter referred to as CG-Zn). The microstructure was studied by combining transmission electron microscopy (TEM), electron backscatter diffraction (EBSD) and X-ray line profile analysis (XLPA). The EBSD and the TEM investigations were performed by a Zeiss Supra 40VP FEG scanning electron microscope and a JEOL-2010 electron microscope at an operating tension of 200 kV, respectively. The X-ray line profiles were measured by a high-resolution rotating anode diffractometer (Nonius, FR 591) using $CuK\alpha_1$ (λ=0.15406 nm) radiation. The line profiles were evaluated by the extended Convolutional Multiple Whole Profile (eCMWP) fitting analysis [4]. As an example, a part of the fitted X-ray diffractogram is shown in Fig. 1a. The CMWP procedure gives the mean crystallite size, the dislocation density, the dislocation contrast factors and the twin boundary frequency. The contrast factors depend on the character of dislocations and therefore enable the determination of the prevailing dislocation slip systems in the specimen [6]. Uniaxial compression tests were conducted over a strain rate range from 6.7×10^{-5} to 6.7×10^{-2} s^{-1} by means of a universal Instron testing machine. Higher strain rates were reached by a direct impact Hopkinson pressure bar (DIHPB) technique [2]. The high temperature mechanical properties of UFG-Zn were studied by indentation creep test using a cylindrical indenter with the diameter of 1.26 mm [7]. The measurements were carried out in the temperature range of 330-359 °C (corresponding to the homologous temperature of 0.87-0.91) and under the stress varied between 35 and 55 MPa.

Results and discussion

Effect of grain size on deformation mechanisms at room temperature. Figs. 1b and 2a show the initial microstructures (before deformation) for UFG- and CG-Zn, respectively. In the UFG-Zn a ZnO phase is formed during the consolidation as revealed by the X-ray diffractogram in Fig. 1a. The ratio of the summed intensities under ZnO and Zn peaks in the diffraction angle range of 30–140° is 9 ± 1 %. The average grain size was 250 nm and 780 μm for the UFG- and CG-Zn samples, respectively.

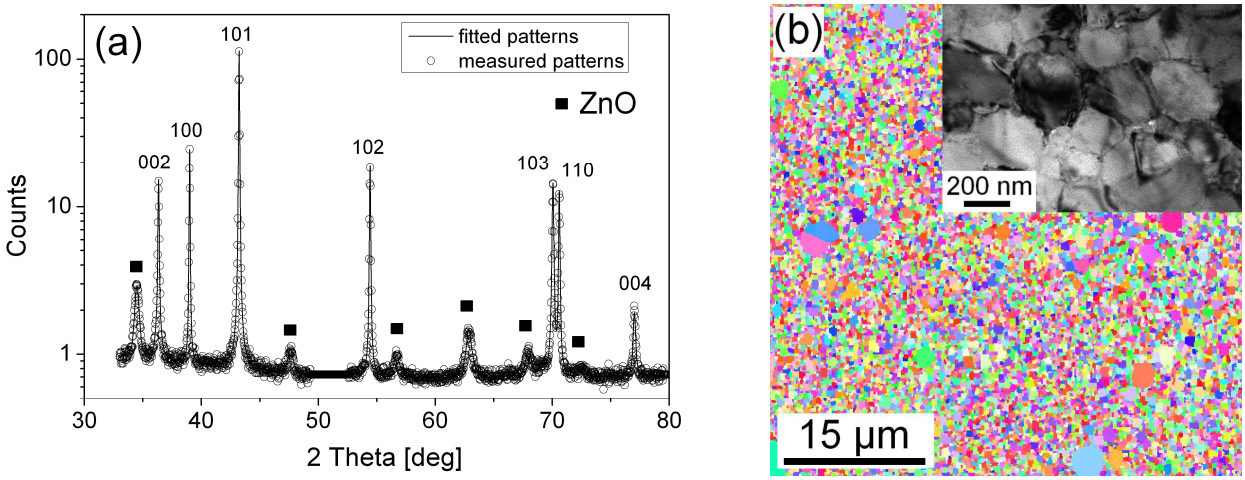

Fig. 1. (a) An X-ray diffractogram and (b) an EBSD image taken on UFG-Zn sample. The inset in (b) shows a TEM picture of the microstructure.

Fig. 3a shows the flow stress versus the strain rate obtained by compression test at room temperature and a strain of 0.05. The flow stress increases with increasing strain rate for both samples reaching values of about 850 MPa and 690 MPa at the highest applied strain rate of ~10^4 s^{-1} for UFG-Zn and CG-Zn, respectively. The flow stress for CG-Zn increases steeply with increasing

strain rate above 10^3 s^{-1}, which is usually explained by the viscous drag of dislocations [1]. For UFG-Zn the steep increase of the flow stress was not observed even at very high strain rates, suggesting that viscous drag effects are negligible for this material. The lack of dislocation drag phenomenon in UFG-Zn can be explained by the relatively large dislocation density (~10^{14} m^{-2}, see below) and the small grain size as both hinder the acceleration of dislocations to very high velocities necessary for the occurrence of viscous drag effects.

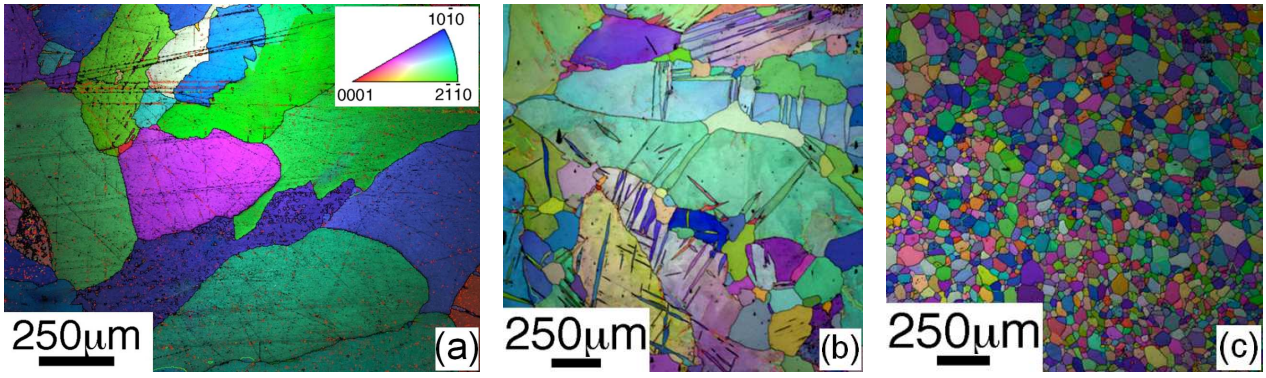

Fig. 2. EBSD images of the (a) initial microstructure, (b) after quasistatic compression (strain rate: 6.7×10^{-4} s^{-1}) and (c) after dynamic compression (strain rate of 9×10^3 s^{-1}) for CG-Zn.

The twin boundary frequency in both the as-consolidated and the compressed UFG-Zn samples was negligible. The dislocation density increases from $0.5 \pm 0.1 \times 10^{14}$ to $1.5 \pm 0.1 \times 10^{14}$ m^{-2} while the crystallite size reduces from 177 ± 17 to 121 ± 13 nm with increasing strain rate from 8×10^{-4} to 3.56 s^{-1}. At high strain rates (10^4 s^{-1}) the dislocation density decreases to $0.8 \pm 0.1 \times 10^{14}$ m^{-2} while the crystallite size increases to 160 ± 17 nm. This can be explained by partial recovery and/or recrystallization. X-ray line profile analysis demonstrated that in the initial state, most of <a> and <c+a> type dislocations are prismatic and pyramidal edge dislocations, respectively. At strain rates higher than 0.35 s^{-1}, in addition to prismatic slip system other <a>-type dislocations in basal and pyramidal slip systems were detected. Similarly, for <c+a>-type dislocations besides pyramidal slip system, prismatic and other pyramidal dislocations were also activated. The ratio of the <a> and <c+a>-type dislocation was 1.8 ± 0.3 irrespectively of the strain rate.

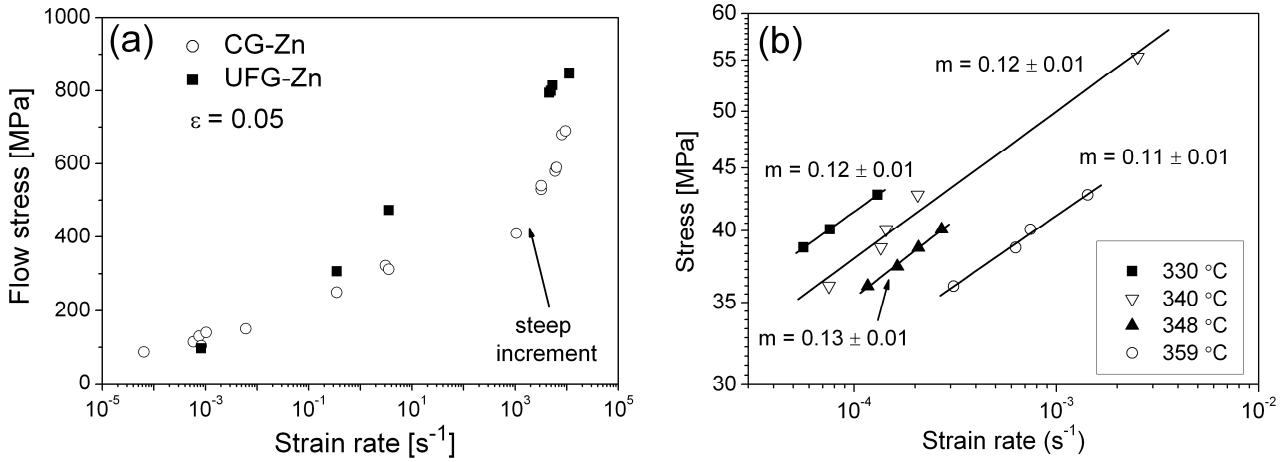

Fig. 3. (a) Flow stress vs. strain rate obtained in compression tests for UFG- and CG-Zn samples. (b) Stress vs. strain rate in double logarithmic scale for UFG-Zn obtained by indentation creep test. The values of the strain rate sensitivity parameter (*m*) are also shows in (b).

The grain size of the CG-Zn sample observed after compression test decreases with increasing rate of deformation (see Figs. 2a-c). At low strain rates many deformation twins were detected (see Fig. 2b) that were not found in the initial unstrained state. As the strain rate increased, the twinning activity decreased. No twins were found after compression tests in the high strain rate regime (see Fig. 2c), where the grain size is lower.

High temperature creep behavior of UFG-Zn. Fig. 3b shows the stress versus strain rate data in double logarithmic scale obtained from high-temperature indentation creep experiments on UFG-Zn. The linear relationship between the logarithm of stress and the logarithm of strain rate suggests that that the deformation is mainly controlled by thermally activated mechanisms. The strain rate sensitivity obtained from the slopes of the straight lines fitted to the data points is 0.12 ± 0.01 which is close to the value of 0.15 determined previously for a Zn sample with the grain size of 238 nm consolidated from ball-milled powder [5]. EBSD and XLPA investigations were performed both inside and outside of the zone indented at 340 ˚C. According to EBSD investigations, the grain sizes in the indented and non-indented volumes are 250 and 280 nm, respectively, which are in good agreement with the grain size of the initial state. XLPA revealed that the twin boundary frequency remained negligible and the dislocation density did not change significantly both inside and outside of the indented zone. In the non-indented volume the types of dislocations also did not change as compared to the initial state. However, in the indented zone additional dislocation slip systems were activated besides prismatic <a> and pyramidal <c+a> dislocations observed in the initial UFG-Zn. Namely, <a>-type basal and pyramidal dislocations as well as other <c+a>-type pyramidal dislocations were formed, indicating a dislocation activity during high temperature creep. Besides dislocation motion, grain boundary sliding may also contribute to plasticity due to the high temperature of deformation (the homologous temperature is 0.87-0.91).

Summary

1) During compression of CG-Zn sample at room temperature and low strain rates, twinning has a considerable contribution to deformation. At the same time, for UFG-Zn the main deformation mechanism is the dislocation motion. The initial UFG-Zn contains mainly prismatic <a> and pyramidal <c+a> dislocations. The compression yields the formation of basal and pyramidal <a> dislocations as well as prismatic and other pyramidal <c+a>-type dislocations.
2) In the case of CG-Zn above the strain rate of 10^3 s^{-1} dislocation drag effects controlled the plasticity. For UFG-Zn the relatively large dislocation density (~10^{14} m^{-2}) and the small grain size (~250 nm) limited the dislocation velocity yielding the lack of dislocation drag effects up to 10^4 s^{-1}.
3) There is a considerable dislocation activity in high-temperature creep of UFG-Zn. Besides prismatic <a> and pyramidal <c+a> dislocations observed in the initial state, <a>-type basal and pyramidal dislocations as well as other <c+a>-type pyramidal dislocations were formed.

Acknowledgements

This work was supported in part by the Hungarian Scientific Research Fund, OTKA, Grant No. K-81360 and the French- Hungarian bilateral project (PHC Balaton, Hungarian Grant No. TeT_10-1-2011-0737).

References

[1] H.J. Frost and M.F. Ashby: *Deformation-mechanism maps* (Pergamon Press, Oxford, New York, 1982).
[2] H. Couque and R. Boulanger, in: *Proceedings of the 23rd International Symposiumon Ballistics*, edited by F. Gáalves and V. Sanchez-Galves, Tarragona, Spain (2007), p. 255
[3] H. Li, Q.Q. Duan, X.W. Li and Z.F. Zhang: Mater. Sci. Eng. A Vol. 466 (2007), p. 38
[4] G. Dirras, J. Gubicza, H. Couque, A. Ouarem and P. Jenei: Mater. Sci. Eng. A Vol. 564 (2013), p. 273
[5] X. Zhang, H. Wang, R.O. Scattergood, J. Narayan, C.C. Koch, A.V. Sergueeva and A.K. Mukherjee: Acta Mater. Vol. 50 (2002), p. 4823
[6] K. Máthis, K. Nyilas, A. Axt, I.C. Dragomir, T. Ungár and P. Lukác: Acta. Mater. Vol. 52 (2004), p. 2889
[7] G. Cseh, N.Q. Chinh, P. Tasnádi and A. Juhász: J. Mater. Sci. Vol. 32 (1997), p. 5107.